Pamukkale Univ Muh Bilim Derg, 28(1), 18-25, 2022

Pamukkale Üniversitesi Mühendislik Bilimleri Dergisi

Pamukkale University Journal of Engineering Sciences

Torsion of variable stiffness composite laminated beams

Değişken rijitlikli kompozit lamine kirişlerin burulması

Muhsin Gökhan GÜNAY[1*]

[1]Department of Mechanical Engineering, Engineering Faculty, Akdeniz University, Antalya, Turkey.
gmgunay@akdeniz.edu.tr

Received/Geliş Tarihi: 04.07.2020 Revision/Düzeltme Tarihi: 06.03.2021 doi: 10.5505/pajes.2021.99404
Accepted/Kabul Tarihi: 16.03.2021 Research Article/Araştırma Makalesi

Abstract

A shear-deformable beam theory is proposed to model the torsional behavior of laminated beams composed of variable stiffness layers. The displacement field is derived by expanding mid-surface displacements in Taylor series in width coordinate and by retaining first-order terms. Stiffness of the beam is made variable by using curvilinear fibers in layers. Variable stiffness layers are categorized into three types as symmetric, asymmetric and anti-symmetric based on their fiber paths. A displacement-based finite element method is used to solve the analytical model and to predict rotations of the beam under torsional load. Beams constructed with symmetric, antisymmetric and asymmetric variable stiffness layers are investigated for several lay-ups by both including and neglecting axial displacement terms. Acquired results are compared with the results of a finite element analysis software. It is observed that the developed model is working properly for beams with variable stiffness layers and including axial displacement terms in calculations improved the model`s performance.

Keywords: Variable stiffness, Curvilinear fibers, Torsion, Laminated beams, Finite element analysis.

Öz

Bu çalışmada değişken rijitlikli katmanlarından oluşan lamine kirişlerin burulma davranışını modellemek için bir kiriş teorisi önerilmiştir. Yer değiştirme alanı, orta yüzey yer değiştirmelerinin enine yönde Taylor serisi ile açılması ve birinci derece terimlerin korunması ile elde edilmiştir. Kirişlerin rijitliği katmanlarda eğrisel elyaflar kullanılarak değişken hale getirilmiştir. Değişken rijitlikli tabakalar elyaf hatlarına göre simetrik, anti-simetrik ve asimetrik olarak üç tipe ayrılmıştır. Analitik modeli çözmek ve kirişlerin yük altında burulmasını tahmin etmek için yer değiştirme tabanlı bir sonlu eleman yöntemi kullanılmıştır. Simetrik, anti-simetrik ve asimetrik değişken rijitlikli katmanlar ile oluşturulan kirişler, çalışmada önemi vurgulanan eksenel yer değiştirme terimlerini dikkate alarak ve ihmal ederek çeşitli katman dizilimleri için incelenmiştir. Elde edilen sonuçlar, sonlu elemanlar analiz yazılımının sonuçları ile karşılaştırılmıştır. Geliştirilen modelin değişken rijitlikli katmanlara sahip kirişler için düzgün çalıştığı ve hesaplamalarda eksenel yer değiştirme terimlerinin modele dahil edilmesinin, modelin performansını artırdığı görülmüştür.

Anahtar kelimeler: Değişken rijitlik, Eğrisel elyaf, Burulma, Lamine kiriş, Sonlu elemanlar yöntemi.

1 Introduction

Today, fiber reinforced composite materials are used in a variety of fields from military applications to commercial products where high strength and lightweight is needed. History of the modern fiber reinforced composites can be dated to 1930s with the first commercial mass production of glass fiber [1]. Fiber reinforced structures are exposed to several types of structural loads during their service time. One of them is torsional loading especially effective on beam like structures. Contemporary studies on torsion of prismatic structures can be traced back to 1850s with Saint Venant`s famous study [2]. Vlasov [3] studied on thin-walled isotropic beams under several loads, and Gjelsvik [4] followed and developed his studies. Bauld and Tzeng [5] adapted Valsov`s study to fiber reinforced thin-walled beams. Massa and Barbero [6] developed a methodology for the analysis of thin-walled composite beams subjected to bending, torque, shear and axial forces. Johnson [7] studied bending and torsion of anisotropic laminated beams. Whitney and Kurtz [8] acquired an exact elasticity solution for the torsion of rectangular plates and investigated shear stresses. Sankar [9] derived a beam theory for torsion of composite beams and investigated beams made up of specially-orthotropic lay-ups. Aldraihem and Wetherhold [10] investigated the coupled bending and twisting vibration in laminated beams depended on Sankar`s formulation and applied finite element method for solution.

Besides the classical straight fibers, curvilinear fibers are used to provided additional opportunities in the design and to improve mechanical performance of composite structures by the new advances in composite production methods such as automated fiber placement (AFP), automated tape laying (ATL) and similar. Kim et. al. developed an experimental setup to variate orientation of tows by continuously shearing them. [11]. Gürdal and Olmedo [12] acquired closed-form and numerical solutions for the elastic response of the composite plates with variable stiffness. While most of the studies on variable stiffness composites investigate plate and cylinder structures there is not that much study on beam structures. Zamani et al. [13] worked on thin-walled beams with bi-convex cross-section and utilized curvilinear fibers to optimize them. Recently, the author of the present work, investigated static behavior of thin-walled composite beams with variable stiffness and thickness [14] and studied their stress distributions along hoop direction [15].

In this study, an analytical model is proposed to predict torsional and flexural behavior of rectangular laminated beams with variable stiffness layers. The displacement field is acquired similar to Sankar`s approach [9] by expanding shear deformable laminated plate theory to Taylor series but different than Sankar additionally axial displacement terms are

*Corresponding author/Yazışılan Yazar

considered. Variable stiffness layers are constructed by using curvilinear fibers and they are categorized into three groups as symmetric, asymmetric and anti-symmetric depended on their shape. The weak formulation of the model is solved by using custom 3 node 13 DOF beam elements. Acquired results of several lay-up cases are compared with the results of a FEA where brick elements are used. Effect of including axial displacement terms into the formulation and effect of different shear coefficient values on the torsion results are investigated.

2 Kinematics

2.1 Displacement field

The displacement field of a laminated plate, whose dimensions are shown in Figure 1, can be expressed as given below by using first-order shear deformation theory.

$$u(x,y,z) = u_0(x,y) + z.\Psi_x(x,y) \quad (1a)$$

$$v(x,y,z) = v_0(x,y) + z.\Psi_y(x,y) \quad (1b)$$

$$w(x,y,z) = w_0(x,y) \quad (1c)$$

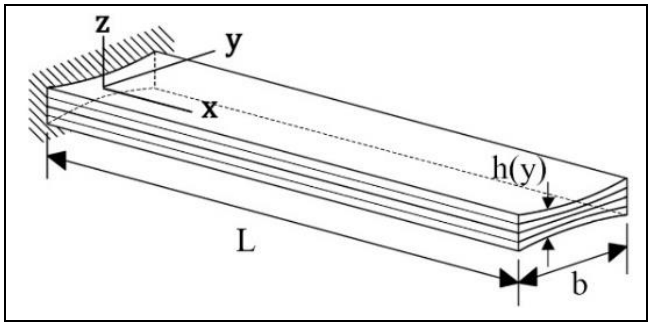

Figure 1. Dimension of laminated beam.

As proposed by Sankar [9] it is possible to expand the displacements given above in Taylor series with respect to the y-axis to investigate torsional-flexural behavior of a laminated beam. By taking zeroth and first-order terms of y in the expansion the assumed displacements given in equations (2a-c) can be acquired as a sum of mid-surface displacement and rotation functions of the beam.

$$u(x,y,z) = U(x) + y.F(x) + z[\phi_x(x) + y.\alpha(x)] \quad (2a)$$

$$v(x,y,z) = V(x) + y.G(x) + z\left[\phi_y(x) + y.\beta(x)\right] \quad (2b)$$

$$w(x,y,z) = W(x) + y.T(x) \quad (2c)$$

Here U and F represent in-plane displacements of the beam in the x-direction, ϕ_x and α represent the rotation of the cross-section about the y-axis, V and G represent in-plane displacements of the beam in the y-direction, ϕ_y and β represent the rotation of the x–z plane about the x-axis, W and T represent the transverse displacement and the twisting angle of the beam centerline, respectively. The displacement and rotation functions of the assumed displacements are shown in Figure 2 in detail.

2.2 Assumptions

The displacements in y-direction ($v_0 = 0 \rightarrow V = G = 0$) and the normal and the shear strains in the y-direction are neglected ($\varepsilon_y = 0 \rightarrow \beta = 0$ and $\gamma_{yz} = 0 \rightarrow \phi_y = -T$). But different from the Sankar`s assumptions the displacements in the x-direction (U and F) are kept. By applying these assumptions, the displacement field takes the form given in equations (3a-c).

$$u = U + y.F + z[\phi_x + y.\alpha] \quad (3a)$$

$$v = -z.T \quad (3b)$$

$$w = W + y.T \quad (3c)$$

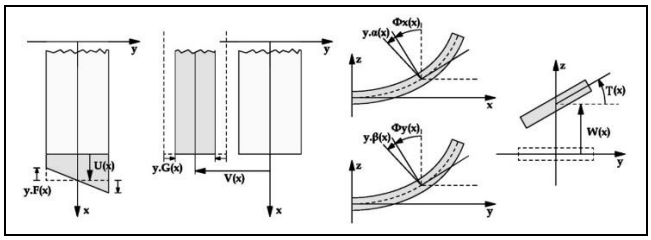

Figure 2. Displacements and rotations of the beam.

2.3 Strain field

The strains are calculated by using infinitesimal strain theory as given below.

$$\varepsilon_x = \frac{\partial u}{\partial x} = U' + y.F' + z[\phi_x' + y.\alpha'] \quad (4a)$$

$$\varepsilon_y = \frac{\partial v}{\partial y} = 0 \quad (4b)$$

$$\varepsilon_z = \frac{\partial w}{\partial z} = 0 \quad (4c)$$

$$\gamma_{xy} = \frac{\partial u}{\partial y} + \frac{\partial v}{\partial x} = F + z[\alpha - T'] \quad (5a)$$

$$\gamma_{xz} = \frac{\partial u}{\partial z} + \frac{\partial w}{\partial x} = \phi_x + W' + y[\alpha + T'] \quad (5b)$$

$$\gamma_{yz} = \frac{\partial v}{\partial z} + \frac{\partial w}{\partial y} = 0 \quad (5c)$$

2.4 Governing equations

Total potential energy of the system is acquired as sum of strain energy and external work.

$$\Pi_{total} = \Pi_{strain} + \mathcal{W}_{ext} \quad (6)$$

In this study stiffness and thickness of the beam depend on the y-axis as will be explained in Section-2.5. Thus, the variation of the stiffness and thickness must be considered while integrating strain energy equation as given below.

$$\Pi_{strain} = \frac{1}{2}\int_0^L \int_{-\frac{b}{2}}^{\frac{b}{2}} \int_{-\frac{h(y)}{2}}^{\frac{h(y)}{2}} [\sigma_x\varepsilon_x + \tau_{xy}\gamma_{xy} + \tau_{xz}\gamma_{xz}]\, dz\, dy\, dx \quad (7)$$

By substituting equations (4a,5a,5b) into equation (7) the strain energy equation is expanded as;

$$\Pi_{strain} = \frac{1}{2}\int_0^L \int_{-\frac{b}{2}}^{\frac{b}{2}} \int_{-\frac{h(y)}{2}}^{\frac{h(y)}{2}} \{\sigma_x[U' + yF' + z(\phi_x' + y\alpha')] + \tau_{xy}[F + z(\alpha - T')] + \tau_{xz}[\phi_x + W' + y(\alpha + T')]\}\, dz\, dy\, dx \quad (8)$$

Then equation (8) is rearranged by expressing force and moment resultants as given below;

$$\Pi_{strain} = \frac{1}{2}\int_0^L \int_{-\frac{b}{2}}^{\frac{b}{2}} \{N_{xx}(y)[U' + yF'] + N_{xy}(y)F + L_{xx}(y)[\phi_x' + y\alpha'] + L_{xy}(y)[\alpha - T'] + Q_x(y)[\phi_x + W' + y(\alpha + T')]\}\, dy\, dx \quad (9)$$

where $N_{xx}(y)$, $N_{xy}(y)$ and $Q_x(y)$ are force resultants, $L_{xx}(y)$ and $L_{xy}(y)$ are moment resultants along thickness as shown in Figure 3 and given in equations (10a-e).

$$N_{xx}(y) = \int_{-\frac{h(y)}{2}}^{\frac{h(y)}{2}} \sigma_x\, dz \quad (10a)$$

$$N_{xy}(y) = \int_{-\frac{h(y)}{2}}^{\frac{h(y)}{2}} \tau_{xy}\, dz \quad (10b)$$

$$L_{xx}(y) = \int_{-\frac{h(y)}{2}}^{\frac{h(y)}{2}} z.\sigma_x\, dz \quad (10c)$$

$$L_{xy}(y) = \int_{-\frac{h(y)}{2}}^{\frac{h(y)}{2}} z.\tau_{xy}\, dz \quad (10d)$$

$$Q_x(y) = \int_{-\frac{h(y)}{2}}^{\frac{h(y)}{2}} \tau_{xz}\, dz \quad (10e)$$

Finally strain energy can be expressed as given below in terms so called beam forces and moments (force and moment resultants across the cross-section) which are given in equations (12a-h).

$$\Pi_{strain} = \frac{1}{2}\int_0^L \left[\bar{N}_x U' + \hat{N}_x F' + \bar{N}_{xy} F + \bar{Q}_x\{W' + \phi_x\} + \hat{Q}_x\{\alpha + T'\} + \bar{M}_x \phi_x' + \hat{M}_x \alpha' + \bar{M}_{xy}\{\alpha - T'\}\right] dx \quad (11)$$

where $\overline{(.)}$ terms indicate the force resultants and $\widehat{(.)}$ or (M) terms indicate the moment resultants across the cross-section as shown below;

$$\bar{N}_x = \int_{-\frac{b}{2}}^{\frac{b}{2}} N_{xx}(y)dy \quad (12a)$$

$$\hat{N}_x = \int_{-\frac{b}{2}}^{\frac{b}{2}} y.N_{xx}(y)dy \quad (12b)$$

$$\bar{N}_{xy} = \int_{-\frac{b}{2}}^{\frac{b}{2}} N_{xy}(y)dy \quad (12c)$$

$$\bar{M}_x = \int_{-\frac{b}{2}}^{\frac{b}{2}} L_{xx}(y)\, dy \quad (12d)$$

$$\hat{M}_x = \int_{-\frac{b}{2}}^{\frac{b}{2}} y.L_{xx}(y)\, dy \quad (12e)$$

$$\bar{M}_{xy} = \int_{-\frac{b}{2}}^{\frac{b}{2}} L_{xy}(y)\, dy \quad (12f)$$

$$\bar{Q}_x = \int_{-\frac{b}{2}}^{\frac{b}{2}} Q_x(y)dy \quad (12g)$$

$$\hat{Q}_x = \int_{-\frac{b}{2}}^{\frac{b}{2}} y.Q_x(y)dy \quad (12h)$$

The external work is done by distributed transverse load $q_z(x,y)$ can be expressed as;

$$\mathcal{W}_{ext} = -\int_0^L \int_{-\frac{b}{2}}^{\frac{b}{2}} [q_z(x,y).w]\, dy\, dx \quad (13)$$

By substituting equation (3c) into equation (13) the work done by external loads is rearranged as;

$$\mathcal{W}_{ext} = -\int_0^L [\bar{q}_z(x).W + \hat{q}_z(x).T]\, dx \quad (14)$$

Where;

$$\bar{q}_z(x) = \int_{-\frac{b}{2}}^{\frac{b}{2}} q_z(x,y)dy \quad (15a)$$

$$\hat{q}_z(x) = \int_{-\frac{b}{2}}^{\frac{b}{2}} y.q_z(x,y)dy \quad (15b)$$

The weak formulation is acquired by equating the variation of the total potential energy to zero,

$$\delta\Pi_{total} = \delta\Pi_{strain} + \delta\mathcal{W}_{ext} = 0 \quad (16)$$

and integrating varied quantities by parts;

$$\int_0^L \left[\bar{N}_x'\delta U + (\hat{N}_x' - \bar{N}_{xy})\delta F + \bar{Q}_x'\delta W + (\hat{Q}_x' - \bar{M}_{xy}')\delta T + (\bar{M}_x' - \bar{Q}_x)\delta\phi_x + (\hat{M}_x' - \hat{Q}_x - \bar{M}_{xy})\delta\alpha + \bar{q}_x.\delta U + \bar{q}_z.\delta W + \hat{q}_z.\delta T\right] dx = 0 \quad (17)$$

Equilibrium equations and natural boundary conditions are expressed as given in Table 1 by collecting coefficients of varied quantities in the weak formulation.

Table 1. Equilibrium equations and Natural boundary conditions

	Equilibrium Eq.s		Natural B.C.s	
δU:	$\bar{N}_x' + \bar{q}_x = 0$	(18a)	$\bar{N}_x\delta U = 0$	(19a)
δF:	$\hat{N}_x' - \bar{N}_{xy} = 0$	(18b)	$\hat{N}_x\delta F = 0$	(19b)
δW:	$\bar{Q}_x' + \bar{q}_z = 0$	(18c)	$\bar{Q}_x\, \delta W = 0$	(19c)
δT:	$Q_x' - \bar{M}_{xy}' + \hat{q}_z = 0$	(18d)	$(\hat{Q}_x - \bar{M}_{xy})\, \delta T = 0$	(19d)
$\delta\phi_x$:	$\bar{M}_x' - \bar{Q}_x = 0$	(18e)	$\bar{M}_x\, \delta\phi_x = 0$	(19e)
$\delta\alpha$:	$\hat{M}_x' - \hat{Q}_x - \bar{M}_{xy} = 0$	(18f)	$\hat{M}_x\, \delta\alpha = 0$	(19f)

2.5 Variable stiffness layers

Stiffnesses of composite layers reinforced with continuous fibers depend on the orientation of the fibers. Orientation variation of the fibers can be controlled by placing curvilinear fibers to follow a specific path. So, stiffness of a layer constructed with curvilinear fibers will vary spatially. To implement variable stiffness layers to the developed model first the variable stiffness layers are defined with three parameters (θ_0, θ_1 and θ_2) on a $\zeta - \eta$ plane and a private name is given for each configuration of these three parameters. Then these named layers are aligned and mapped to the desired section and layer of the laminated beam. An example of this procedure is shown in Figure 3.

The orientation angle of curvilinear fibers is linearly varied and defined depended on ζ axis as;

$$\theta(\zeta) = \begin{cases} (\theta_1 - \theta_0).\zeta + \theta_1, & -1 \le \zeta \le 0 \\ (\theta_2 - \theta_1).\zeta + \theta_1, & 0 < \zeta \le 1 \end{cases} \quad (20)$$

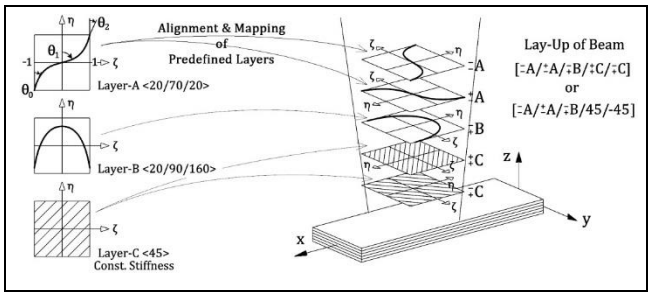

Figure 3. Alignment & mapping of variable stiffness layers.

And the function describing the fiber path (shape of curvilinear fiber) which is having the orientation angle variation expressed above is acquired as given below.

For $-1 \le \zeta \le 0$;

$$\eta(\zeta) = \frac{-ln\left[cos\left((\theta_0-\theta_1).\zeta+90-\theta_1\right)\right]+ln[cos(90-\theta_1)]}{\pi.\frac{(\theta_0-\theta_1)}{180}} \quad (21a)$$

For $0 \le \zeta \le 1$;

$$\eta(\zeta) = \frac{-\ln\left[\cos\left((\theta_1-\theta_2).\zeta+90-\theta_1\right)\right]+\ln[\cos(90-\theta_1)]}{\pi.\frac{(\theta_1-\theta_2)}{180}} \quad (21b)$$

where θ_0, θ_1 and θ_2 expresses the orientations at $\zeta = -1$, origin and $\zeta = 1$ respectively. θ_0, θ_1 and θ_2 can be chosen between 0^o and 180^o as a clock-wise angle from $\eta(+)$ direction to the orientation of fiber path. Any combination of θ_0, θ_1 and θ_2 parameters are called as configuration and shown by $\langle \theta_0/\theta_1/\theta_2 \rangle$ notation.

Production of variable stiffness layers with curvilinear fibers is not discussed in this paper, methods such as automated fiber placement (AFP), automated tape laying (ATL), Continuous tow shearing method [15] can be used for this purpose. It is assumed that the variable stiffness layers do not have any gap or overlap and the curved fibers are placed by shifting the fiber path along η axis. This makes the stiffness of the layer constant along η axis and varying along ζ axis. Producing the layers with the curved fibers causes the thickness to change in the layers depending on the orientation variation. The thickness variation of the layer is modelled similar to [11] as given below:

$$h(\zeta) = \frac{h_0}{\cos(\theta(\zeta)-\theta_{ref})} \quad (22)$$

where θ_{ref} is the orientation where the thickness of the layer equals the original thickness h_0.

The $\zeta-\eta$ plane can be aligned with (x,y,z) local coordinate system by matching ζ-axis with y-axis and η-axis with the x-axis. By flipping $\zeta-\eta$ plane alignment of variable stiffness layers can be done in four different ways as presented in Figure 4. Symbolic presentation of alignments for layer-a are expressed with $\binom{(\eta)}{(\zeta)}\boldsymbol{a}$, where (+) means default (not flipped) direction, and (-) means reversed (flipped) direction of the corresponding axis.

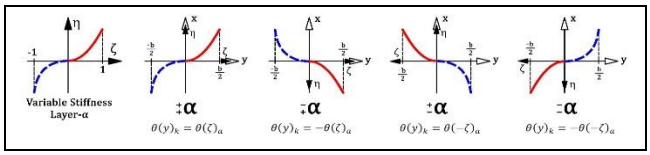

Figure 4. Mapping variable stiffness layer a to k^{th} layer of the laminated beam. $\left(\frac{-b}{2} \le y \le \frac{b}{2}\right)$ and $(-1 \le \zeta \le 1)$.

After mapping elements of A(y), B(y), D(y) matrices can be calculated depending on variable $\theta(y)_k$ as given below:

$$A_{ij}(y) = \sum_{k=1}^{N} \bar{q}_{ij}(\theta(y)_k).\left(n_k(y)-n_{k-1}(y)\right) \quad (23a)$$

$$B_{ij}(y) = \frac{1}{2}\sum_{k=1}^{N} \bar{q}_{ij}(\theta(y)_k).\left(n_k^2(y)-n_{k-1}^2(y)\right) \quad (23b)$$

$$D_{ij}(y) = \frac{1}{3}\sum_{k=1}^{N} \bar{q}_{ij}(\theta(y)_k).\left(n_k^3(y)-n_{k-1}^3(y)\right) \quad (23c)$$

here $n_k(y)$ terms will be depended on the thickness variation of layers. $A_{55}(y)$ is scaled by multiplying itself with shear correction factor ($\mathcal{K}$). Effects of different values of shear correction factor are investigated and discussed in the numerical results section.

2.6 Classification of variable stiffness layers

Variable stiffness layers defined by equations (20, 21) can be classified based on the shape of the fiber path as symmetric and antisymmetric corresponding to the cases of $< \theta_1 = 90^o, \theta_2 = 180^o - \theta_0 >$ and $<\theta_0 = \theta_2>$ respectively. All the other remaining configurations of θ_0, θ_1 and θ_2 will give an asymmetric variable stiffness layer. Each of these three types of variable stiffness layers are illustrated in Figure 5.

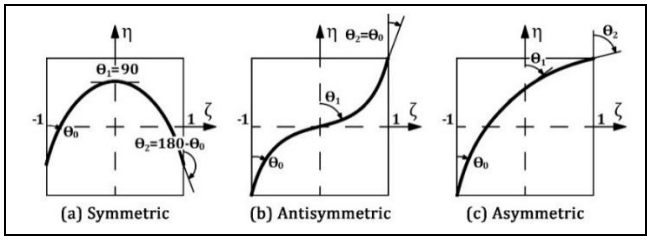

Figure 5. Classification of variable stiffness layers by fiber path shape.

2.7 Constitutive equations

The constitutive relations between stresses and strains of the beam composed of variable stiffness layers can be defined as follows, where stiffness elements are variable along y-axis dependent on the variable fiber orientation angle $\theta(y)$.

$$\begin{Bmatrix}\sigma_x\\ \tau_{xy}\\ \tau_{xz}\end{Bmatrix}^k = \begin{bmatrix}\bar{q}_{11}(\theta(y)) & \bar{q}_{16}(\theta(y)) & 0\\ \bar{q}_{16}(\theta(y)) & \bar{q}_{66}(\theta(y)) & 0\\ 0 & 0 & \bar{q}_{55}(\theta(y))\end{bmatrix}^k . \begin{Bmatrix}\varepsilon_x\\ \gamma_{xy}\\ \gamma_{xz}\end{Bmatrix} \quad (24)$$

The constitutive relations can be obtained by substituting first equation (24) into equations (10a-e) then equations (10a-e) into equations (12a-h) as given below;

$$\begin{Bmatrix} \bar{N}_x \\ \hat{N}_x \\ \bar{N}_{xy} \\ \bar{M}_x \\ \hat{M}_x \\ \bar{M}_{xy} \\ \bar{Q}_x \\ \hat{Q}_x \end{Bmatrix} = [e_{ij}]_{8x8} \cdot \begin{Bmatrix} U' \\ F' \\ F \\ \phi_x{}' \\ \alpha' \\ \alpha - T' \\ W' + \phi_x \\ \alpha + T' \end{Bmatrix} \quad (25)$$

where $[e_{ij}]$ matrix is called as beam stiffness matrix and elements of the beam stiffness matrix are presented in appendix-A.

If U and F displacements are ignored and taken as zero the first three row and column of $[e_{ij}]$ matrix vanishes and the size of the matrix reduces to 5 by 5. And also if D_{ij} and A_{55} is constant e_{45} and e_{56} will vanish and the formulation reduces to the form proposed by Sankar [9].

In the formulation, it is seen that the W displacement is directly coupled with the ϕ_x displacement, and similarly α is coupled with T. But the deflection (W) and the rotation (T) will not be coupled unless e_{45} or e_{78} is different than zero. For layers having variable stiffness and thickness the value of e_{45} or e_{78} will depend on the configuration, alignment and lay-up of variable stiffness layers.

2.8 Finite element formulation

The solution of the developed model is achieved by using a displacement-based finite element method by using 3-node 13-DOF finite beam elements shown in Figure 6. Displacement terms are discretized as given in equations (26a-f) where W displacement is represented with 3 nodes and others with 2 nodes. Shape function S_w is selected as three node linear interpolation function and other shape functions are selected as two node linear interpolation function.

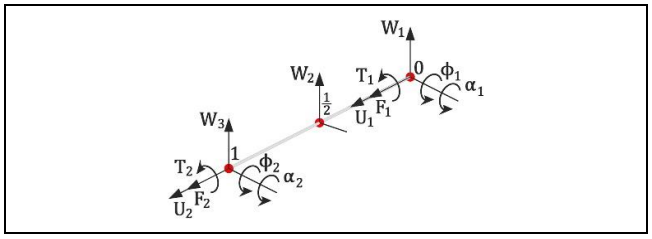

Figure 6. Finite beam element (3 node 13 DOF).

$$U \cong \sum_{i=1}^{n} S_U . U_i \quad (26a)$$

$$F \cong \sum_{i=1}^{n} S_F . F_i \quad (26b)$$

$$W \cong \sum_{i=1}^{n} S_w . W_i \quad (26c)$$

$$T \cong \sum_{i=1}^{n} S_T . T_i \quad (26d)$$

$$\phi \cong \sum_{i=1}^{n} S_\phi . \phi_i \quad (26e)$$

$$\alpha \cong \sum_{i=1}^{n} S_\alpha . \alpha_i \quad (26f)$$

The constitutive relations given in equation (25) is submitted into the weak formulation presented in equation (17) and by the use of discretized displacements given above the following finite element formulation is acquired.

$$[k].\{u\} = \{f\} \quad (27)$$

$$\begin{bmatrix} k_{11} & k_{12} & k_{13} & k_{14} & k_{15} & k_{16} \\ & k_{22} & k_{23} & k_{24} & k_{25} & k_{26} \\ & & k_{33} & k_{34} & k_{35} & k_{36} \\ & & & k_{44} & k_{45} & k_{46} \\ & sym & & & k_{55} & k_{56} \\ & & & & & k_{66} \end{bmatrix} \cdot \begin{Bmatrix} U_i \\ F_i \\ W_i \\ T_i \\ \phi_i \\ \alpha_i \end{Bmatrix} = \begin{Bmatrix} f_U \\ 0 \\ f_W \\ f_T \\ 0 \\ 0 \end{Bmatrix} \quad (28)$$

where [k] is local stiffness matrix, $\{u\}$ is local displacement vector and $\{f\}$ is local force vector. Elements of [k] and $\{f\}$ are presented in terms of elements of $[e_{ij}]$ beam stiffness matrix as are given in appendix-B.

3 Numerical results

In this section, fixed free beams composed of symmetric, antisymmetric and asymmetric variable stiffness layers are investigated. The beams are constructed by using four variable stiffness layers and loaded with a torsional load of 5 Nm at the free tip. Rotation of the free tip is calculated for several lay-up cases with the developed model both including and ignoring (U and F) displacement functions. Also, the effect of two different shear correction factor values (K=5/6 and K=1/6) are investigated. For validation, results of the developed model are compared with the results of a finite element analysis by using 20-node brick elements with reduced integration where the beam is modeled with 750 x 100 x 4 elements. Orientation angles and thicknesses of each layer of each brick elements are adjusted to imitate orientation and thickness variation of variable stiffness layers. Material properties of the carbon-epoxy composite used at the layers are given in Table 2 and dimensions of the investigated beams are shown in Figure 7. The original thickness (h_0) of each variable stiffness layer is taken as 1 mm.

Table 2. Mechanical properties of composite material.

E_1	E_2	G_{12}	ν_{12}
145 [GPa]	10 [GPa]	5 [GPa]	0.32

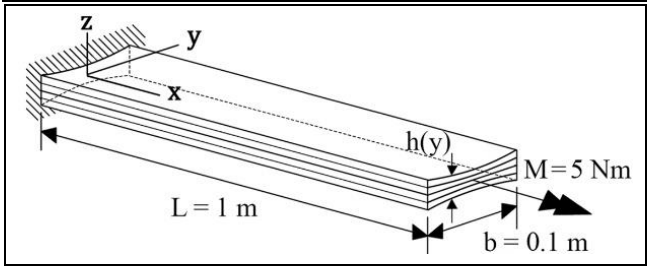

Figure 7. Loading case.

In the following figures results are labeled as "FEA" for brick element based finite element analysis, as "Present (K=1/6)" for present calculation where U and F displacements are included and K is chosen as 1/6, as "Present (K=5/6)" for present calculation where U and F displacements are included and K is chosen as 5/6 and as "Present (U=F=0)" for present calculation where U and F displacements are neglected and K is chosen as 5/6, respectively.

3.1 Beams with symmetric variable stiffness layers

As presented in Section 2.6 a symmetric variable stiffness layer can be defined by taking θ_1=90^0 and $\theta_2 = 180^0 - \theta_0$. The beam which is constructed by using the "symmetric variable stiffness layer-A" with $[\ddagger A/\mp A/\ddagger A/\mp A]$ lay-up is investigated by increasing θ_0 from 5^0 to 85^0 by a step of 5^0. The axial rotation results of the free tip are given in Figure 8.

3.2 Beams with antisymmetric variable stiffness layers

Similar to the previous case, this time by using an antisymmetric variable stiffness layer, the beam with $[\ddagger B/\mp B/\ddagger B/\mp B]$ lay-up is investigated by increasing θ_0 from 5^0 to 85^0 by a step of 5^0. The antisymmetric variable stiffness layer-B used in lay-ups is defined by taking $\theta_2 = \theta_0$ and $\theta_1 = 90^0 - \theta_0$. The axial rotation results of the free tip are given in Figure 9 for$[\ddagger B/\mp B/\ddagger B/\mp B]$ lay-up case.

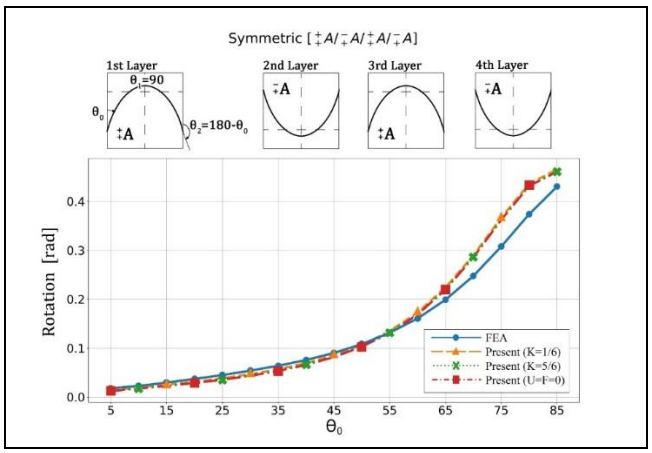

Figure 8. Rotation of free tip for $[\ddagger A/\mp A/\ddagger A/\mp A]$ lay-up with symmetric variables stiffness layers.

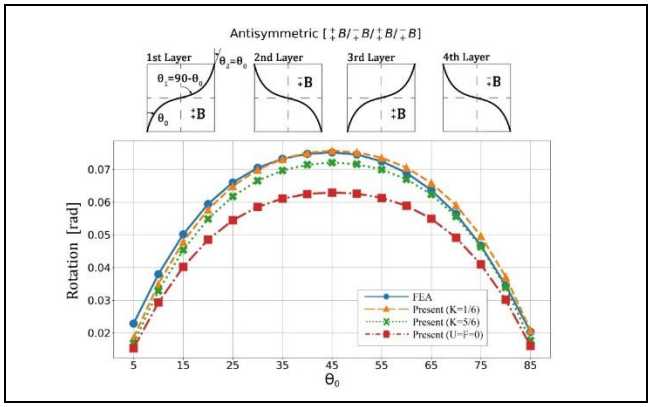

Figure 9. Rotation of free tip for $[\ddagger B/\mp B/\ddagger B/\mp B]$ lay-up with antisymmetric variables stiffness layers.

3.3 Beams with asymmetric variable stiffness layers

Any other selection of θ_0, θ_1 and θ_2 expect symmetric and antisymmetric configurations will cause an asymmetric variable stiffness layer configuration. In this section two different beams composed of asymmetric variable stiffness layers with $[\ddagger C/\mp C/\ddagger C/\mp C]$ and $[\ddagger C/\pm C/\ddagger C/\pm C]$ lay-up cases are investigated, where last lay-up case is a non-classical lay-up where the layers are flipped around ζ-axis or η-axis as presented previously in Figure 4. The asymmetric variable stiffness layer-C used in lay-ups is defined by taking $\theta_2 = 90^0 - \theta_0$ and $\theta_1 = 45^0$. The axial rotation results of the free tip are given in Figures 10 and 11, respectively for $[\ddagger C/\mp C/\ddagger C/\mp C]$ and $[\ddagger C/\pm C/\ddagger C/\pm C]$ lay-up cases. At $[\ddagger C/\mp C/\ddagger C/\mp C]$ lay-up case a weak coupling between rotation and deflection is observed.

3.4 Discussion of results

It is seen at Figures 8-11 that calculated results have same characteristics with FEA results. At Figure 8 torsion increases as θ_0 increase. Taking $\theta_0 = 45^0$ makes both θ_1 and θ_2 to be equal to 45^0 and gives conventional straight fibers for layers B and C. It is also seen that at Figures 9-11 torsion takes its maximum value for $\theta_0 = 45^0$ then gradually descends towards both left and right. It must be noted that the variation of thickness is effective as well as the variation of stiffness on the behavior of the beam.

Including U-F displacements terms in calculations improved the model`s performance expect $[\ddagger A/\mp A/\ddagger A/\mp A]$ lay-up case (Figure 8) where both calculated results with and without U-F terms have similar values. In all calculations almost the same torsional results with FEA results are acquired by taking shear correction factor as 1/6 instead of classic 5/6 value.

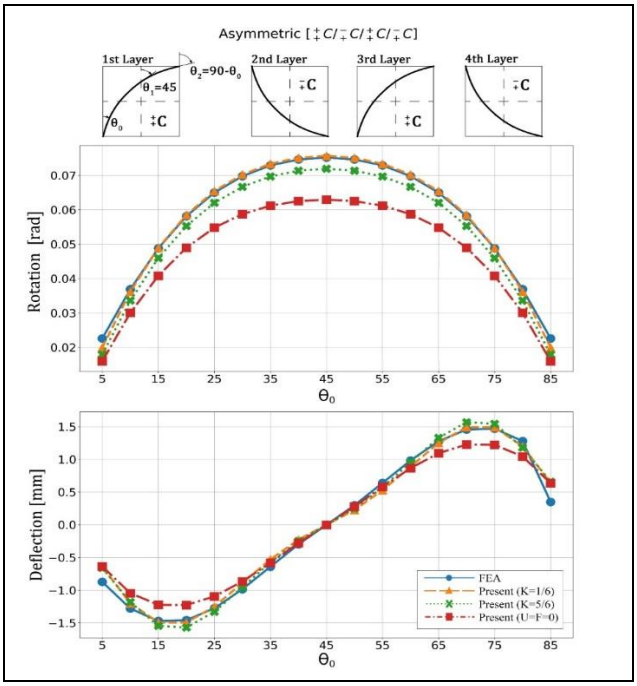

Figure 10. Rotation and deflection of free tip for $[\ddagger C/\mp C/\ddagger C/\mp C]$ lay-up with symmetric variables stiffness layers.

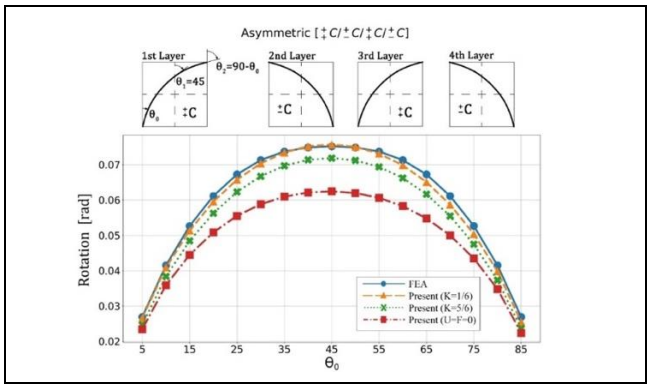

Figure 11. Rotation of free tip for $[\ddagger C/\pm C/\ddagger C/\pm C]$ lay-up with symmetric variables stiffness layers.

The e_{46} or e_{78} terms are acquired as zero for $[\overset{+}{+}A/\overset{-}{+}A/\overset{+}{+}A/\overset{-}{+}A]$, $[\overset{+}{+}B/\overset{-}{+}B/\overset{+}{+}B/\overset{-}{+}B]$ and $[\overset{+}{+}C/\overset{-}{+}C/\overset{+}{+}C/\overset{-}{+}C]$ lay-up cases and any coupling between rotation and displacement does not occur for these calculations as expected and previously discussed in section 2.7. On the other hand, for $[\overset{+}{+}C/\overset{-}{+}C/\overset{+}{+}C/\overset{-}{+}C]$ lay-up case (Figure 10) e_{46} and e_{78} terms are not zero and a weak coupling between rotation and displacement is observed.

4 Conclusion

An analytical model is developed to investigate the torsional behavior of beams composed of variable stiffness layers. Variable stiffness layers are categorized into three groups as symmetric, antisymmetric and asymmetric. Fixed free beams are constructed by using three type of variable stiffness layers proposed and loaded with a torsional load at the free end. The rotation and deflection values of the free end are acquired with the developed model by including and neglecting axial displacement terms (U and F). The model proposed by Sankar can be achieved as a special case of the present model when the axial displacement terms are ignored. The results of the present model are compared with the results of a finite element analysis where brick elements are used. It is observed that including axial displacement terms (U and F) in calculations is increased model`s performance.

5 Author contribution statements

The study is prepared by the author Muhsin Gökhan GÜNAY only.

6 Ethics committee approval and conflict of interest statement

There is no need to obtain permission from the ethics committee for the article prepared. There is no conflict of interest with any person/institution in the article prepared.

7 References

[1] Loewenstein KL. *The Manufacturing Technology of Continuous Glass Fibers*. 3rd ed. New York, USA, Elsevier Scientific, 1973.

[2] Saint-Venant. *Mémoire Sur la Torsion des Prismes*. Paris, France, Imprimerie Nationale 1856.

[3] Vlasov VZ. *Thin Walled Elastic Beams.* 2nd ed. Jerusalem, Israea, Israel Program for Scientific Transactions, 1961.

[4] Gjelsvik A. *The Theory of Thin Walled Bars*. 1st ed. New York, USA, Wiley, 1981.

[5] Bauld Jr NR and Tzeng LS. "A Vlasov theory for fiber-reinforced beams with thin-walled open cross sections". *International Journal of Solids and Structures*, 20(3), 277-297, 1984.

[6] Barbero EJ, Massa JC. "A strength of materials formulation for thin walled composite beams with torsion". *Journal of Composite Materials*, 32, 1560-1594, 1998.

[7] Johnson AF. "Bending and torsion of anisotropic beams", *International Journal of Solids and Structures*, 9(4), 527-551, 1973.

[8] Whitney JM, Kurtz RD. "Analysis of orthotropic laminated plates subjected to torsional loading". *Composites Engineering*, 3(1), 83-97, 1993.

[9] Sankar BV. "A beam theory for laminated composites and application to torsion problems". *Journal of Applied Mechanics*, 60(1), 246-249, 1993.

[10] Aldraihem OJ, Wetherhold RC. "Mechanics and control of coupled bending and twisting vibration of laminated beams". *Smart Materials and Structures*, 6(2), 123-133, 1997.

[11] Kim BC, Weaver PM, Potter K. "Manufacturing characteristics of the continuous tow shearing method for manufacturing of variable angle tow composites." *Composites Part A*, 61, 141-151, 2014.

[12] Gürdal Z, Olmedo R. "In-plane response of laminates with spatially varying fiber orientations: Variable stiffness concept". *AIAA Journal*, 31(4), 751-758, 1993.

[13] Zamani Z, Haddadpour H, Ghazavi MR, "Curvilinear fiber optimization tools for design thin-walled beams". *Thin Walled Structures*, 49(3), 448-454, 2011.

[14] Günay MG, Timarci T. "Static analysis of thin-walled laminated composite closed section beams with variable stiffness". *Composite Structures*, 182, 67-78, 2017.

[15] Günay MG, Timarci T. "Stresses in thin-walled composite laminated box-beams with curvilinear fibers: Antisymmetric and symmetric fiber paths". *Thin Walled Structures*, 138, 170-182, 2019.

Appendix A

Elements of beam stiffness matrix $[e_{ij}]$.

$$e_{11} = \int_{-\frac{b}{2}}^{\frac{b}{2}} A_{11}(y)dy$$

$$e_{12} = \int_{-\frac{b}{2}}^{\frac{b}{2}} y.A_{11}(y)dy$$

$$e_{13} = \int_{-\frac{b}{2}}^{\frac{b}{2}} A_{16}(y)dy$$

$$e_{14} = \int_{-\frac{b}{2}}^{\frac{b}{2}} B_{11}(y)dy$$

$$e_{15} = \int_{-\frac{b}{2}}^{\frac{b}{2}} y.B_{11}(y)dy$$

$$e_{16} = \int_{-\frac{b}{2}}^{\frac{b}{2}} B_{16}(y)dy$$

$$e_{22} = \int_{-\frac{b}{2}}^{\frac{b}{2}} y^2.A_{11}(y)dy$$

$$e_{23} = \int_{-\frac{b}{2}}^{\frac{b}{2}} y.A_{16}(y)dy$$

$$e_{24} = \int_{-\frac{b}{2}}^{\frac{b}{2}} y.B_{11}(y)dy$$

$$e_{25} = \int_{-\frac{b}{2}}^{\frac{b}{2}} y^2.B_{11}(y)dy$$

$$e_{26} = \int_{-\frac{b}{2}}^{\frac{b}{2}} y.B_{16}(y)dy$$

$$e_{33} = \int_{-\frac{b}{2}}^{\frac{b}{2}} A_{66}(y)dy$$

$$e_{34} = \int_{-\frac{b}{2}}^{\frac{b}{2}} B_{16}(y)dy$$

$$e_{35} = \int_{-\frac{b}{2}}^{\frac{b}{2}} y.B_{16}(y)dy$$

$$e_{36} = \int_{-\frac{b}{2}}^{\frac{b}{2}} B_{66}(y)dy$$

$$e_{44} = \int_{-\frac{b}{2}}^{\frac{b}{2}} D_{11}(y)dy$$

$$e_{45} = \int_{-\frac{b}{2}}^{\frac{b}{2}} y.D_{11}(y)dy$$

$$e_{46} = \int_{-\frac{b}{2}}^{\frac{b}{2}} D_{16}(y)dy$$

$$e_{55} = \int_{-\frac{b}{2}}^{\frac{b}{2}} y^2.D_{11}(y)dy$$

$$e_{56} = \int_{-\frac{b}{2}}^{\frac{b}{2}} y.D_{16}(y)dy$$

$$e_{66} = \int_{-\frac{b}{2}}^{\frac{b}{2}} D_{66}(y)dy$$

$$e_{77} = \int_{-\frac{b}{2}}^{\frac{b}{2}} A_{55}(y)dy$$

$$e_{78} = \int_{-\frac{b}{2}}^{\frac{b}{2}} y.A_{55}(y)dy$$

$$e_{88} = \int_{-\frac{b}{2}}^{\frac{b}{2}} y^2.A_{55}(y)dy$$

Other terms are zero.

Appendix B

Elements of local stiffness matrix $[k_{ij}]$ and local force vector $\{f\}$.

$$k_{11} = \int_0^{\ell} e_{11}.S'_U.S'_U\,dx$$

$$k_{12} = \int_0^{\ell} e_{12}.S'_U.S'_F\,dx$$

$$k_{14} = -\int_0^{\ell} e_{16}.S'_U.S'_T\,dx$$

$$k_{15} = \int_0^{\ell} e_{14}.S'_U.S'_\phi\,dx$$

$$k_{16} = \int_0^{\ell} e_{15}.S'_U.S'_\alpha\,dx$$

$$k_{22} = \int_0^{\ell} e_{22}.S'_F.S'_F - e_{33}.S_F.S_F\,dx$$

$$k_{24} = -\int_0^{\ell} e_{26}.S'_F.S'_T\,dx$$

$$k_{25} = \int_0^{\ell} e_{24}.S'_F.S'_\phi\,dx$$

$$k_{26} = \int_0^{\ell} e_{25}.S'_F.S'_\alpha - e_{25}.S_F.S_\alpha\,dx$$

$$k_{33} = \int_0^{\ell} e_{77}.S'_W.S'_W\,dx$$

$$k_{34} = \int_0^{\ell} e_{78}.S'_W.S'_T\,dx$$

$$k_{44} = \int_0^{\ell} (e_{66} + e_{88}).S'_T.S'_T\,dx$$

$$k_{45} = -\int_0^{\ell} e_{46}.S'_T.S'_\phi\,dx$$

$$k_{46} = -\int_0^{\ell} e_{56}.S'_T.S'_\alpha\,dx$$

$$k_{55} = \int_0^{\ell} e_{44}.S'_\phi.S'_\phi - e_{77}.S_\phi.S_\phi dx$$

$$k_{56} = \int_0^{\ell} e_{45}.S'_\phi.S'_\alpha - e_{78}.S_\phi.S_\alpha dx$$

$$k_{66} = \int_0^{\ell} e_{55}.S'_\alpha.S'_\alpha - (e_{66} + e_{88}).S_\alpha.S_\alpha dx$$

$$f_U = \int_0^{\ell} q_{x,i}.S_U\,dx$$

$$f_W = \int_0^{\ell} \bar{q}_{z,i}.S_w\,dx$$

$$f_T = \int_0^{\ell} \hat{q}_{z,i}.S_T\,dx$$

Other terms are zero.